IEEE Photonics Journal
An IEEE Photonics Society Publication

Open Access

# The Effect of Tensile Strain on Optical Anisotropy and Exciton of *m*-Plane ZnO

Volume 7, Number 2, April 2015

H. H. Wang
J. S. Tian
C. Y. Chen
H. H. Huang
Y. C. Yeh
P. Y. Deng
L. Chang
Y. H. Chu
Y. R. Wu
J. H. He

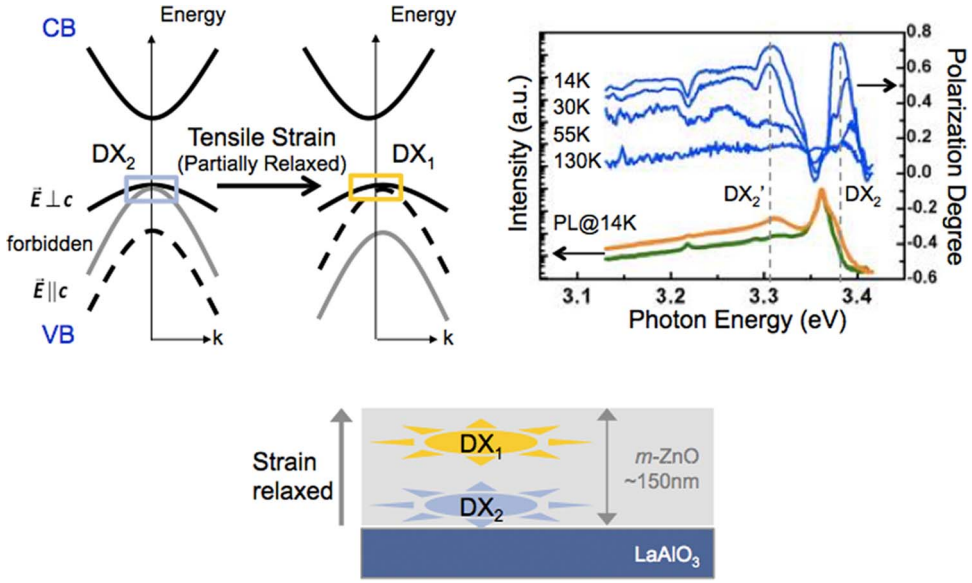


DOI: 10.1109/JPHOT.2015.2415672


IEEE photonics SOCIETY

IEEE

# The Effect of Tensile Strain on Optical Anisotropy and Exciton of *m*-Plane ZnO

**H. H. Wang,[1] J. S. Tian,[2] C. Y. Chen,[1] H. H. Huang,[3] Y. C. Yeh,[2] P. Y. Deng,[3] L. Chang,[2] Y. H. Chu,[2] Y. R. Wu,[3] and J. H. He[1]**

[1]Computer, Electrical and Mathematical Sciences and Engineering Division, King Abdullah University of Science and Technology, Thuwal 23955-6900, Saudi Arabia
[2]Department of Materials Science and Engineering, National Chiao Tung University, Hsinchu 300, Taiwan
[3]Institute of Photonics and Optoelectronics and Department of Electrical Engineering, National Taiwan University, Taipei 10617, Taiwan

*DOI: 10.1109/JPHOT.2015.2415672*


Manuscript received February 25, 2015; revised March 12, 2015; accepted March 15, 2015. Date of publication March 20, 2015; date of current version April 1, 2015. Corresponding author: J. H. He (e-mail: jrhau.he@kaust.edu.sa).

**Abstract:** The near band edge emission of the tensile-strained *m*-plane ZnO film grown on (112)$LaAlO_3$ substrates shows abnormal low polarization degree ($\rho = 0.1$). The temperature dependency of polarization degree clarifies the origins of different emission peaks. In tensile-strained m-plane ZnO, the [0001] polarized state is upper shifted and is overlapping with the [11$\bar{2}$0] polarized state. This phenomenon causes the abnormal low polarization degree and reveals the effect of strain on the emission anisotropy of *m*-plane ZnO.

**Index Terms:** Optical films, photoluminescence, optical polarization, strain, II-VI semiconductor materials.

## 1. Introduction

ZnO, which is known to be a wide band gap material with high exciton binding energy, is a promising material for optoelectronic devices [1], [2]. For light-emitting applications, quantum wells (QWs) in light emission devices can effectively increase the emission efficiency. Unfortunately, similar to *c*-plane GaN QWs, *c*-plane ZnO QW structures also suffers from the intrinsic internal electric field that leads to the spatial separation of the wave functions of electron and hole, which causes the decrease in transition efficiency [3]. To boost the emission efficiency *via* eliminating the internal field in QWs, the non-polar ZnO QW, i.e., *m*-plane or *a*-plane, has attracted considerable attention [4], [5].

The polarization anisotropy in light emission is another feature of the non-polar ZnO-based light emitting device, which originates from the band splitting of the valence bands (VBs) in wurtzite ZnO. However, a polarized light source is sometimes highly undesirable in a certain optical system, including an optical communication system, an interferometer, and sensors [6], [7]. Therefore, the management of polarization anisotropy is critical to achieve light source with desired properties. Previously, it has been demonstrated that under a strong compressive strain, the polarization anisotropy of ZnO films is distinct from bulk ZnO and the reordering of VBs is observed [8], [9]. Nevertheless, the optical characteristics of non-polar ZnO films under tensile strain remain unclear since the sapphire, which is the most commonly used substrate to grow

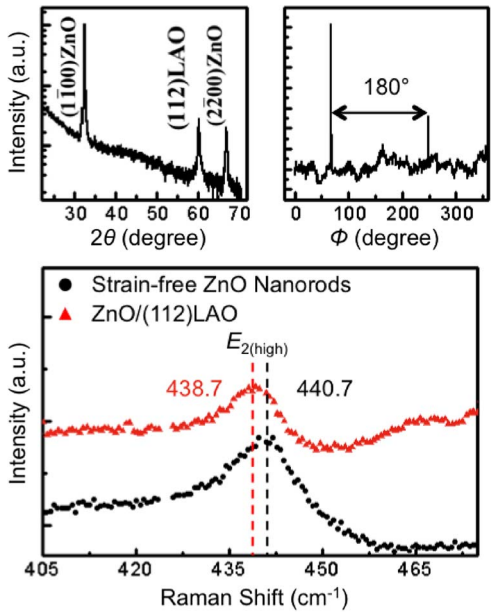


Fig. 1. X-ray diffraction pattern of (a) $\theta$–$2\theta$ and (b) in-plane $\phi$ scan of ZnO film grown on (112)LAO. (c) Raman spectra of m-plane ZnO film grown on (112)LAO (red) and strain free ZnO nanorods (black).

non-polar ZnO films, usually results in compressive strain. Recently, $LaAlO_3$ (LAO) has been newly developed as a substrate to grow non-polar ZnO films because of its small lattice mismatch comparing to sapphire, thermal stability and potential to integrate ZnO with Si[8]. According to the lattice mismatch of 2.8% $(\|c)$ and 1.0% $(\perp c)$ between *m*-plane ZnO and (112)LAO, tensile strain is expected. Accordingly, the optical characterization on *m*-plane ZnO films grown on (112)LAO under tensile strain can not only help us evaluate the feasibility of this new substrate, but also expand our general understanding of the optical property of tensile-strained ZnO. In this work, the tensile strain-induced reordering of VBs and the related strain relaxation are found to result in weakened optical anisotropy in *m*-plane ZnO on (112)LAO by measuring temperature- and polarization-dependent photoluminescence (PL) spectra and simulation, which employs the $k \bullet p$ method and is performed to confirm the experimental result.

## 2. Experimental Detail

The *m*-plane ZnO film was grown on (112)LAO using laser molecular beam epitaxy with a KrF excimer laser $(\lambda = 248\ \text{nm})$. The microstructure characteristics and strain condition were investigated by X-ray diffraction (XRD) and the Raman spectroscopy, respectively. The Raman spectrum was measured by a Jobin Yvon T64000 triple spectrometer equipped with a charged-coupled device cooled at 160 K. The temperature dependent PL spectra were obtained by using an He-Cd laser $(\lambda = 325\ \text{nm})$ with the laser power density of 0.8 W/cm$^2$ as the excitation source. For polarization-dependent PL, we placed a polarizer in front of the monochromator and calibrated the system in order to reduce the polarization dependency caused by the instrument itself.

## 3. Material Growth and Structural Analysis

For the growth of non-polar m-plane ZnO, we choose a (112)LAO substrate which can be considered as a 35.26° miscut of (001) along [110]LAO. The (112) surface of LAO with rectangular template of 5.36 Å x 6.57 Å gives the lattice mismatch of 2.8% $(//c)$ and 1.0% $(\perp c)$ with ZnO [8]. To investigate the crystallinity of the as-grown ZnO films on (112)LAO, we performed the

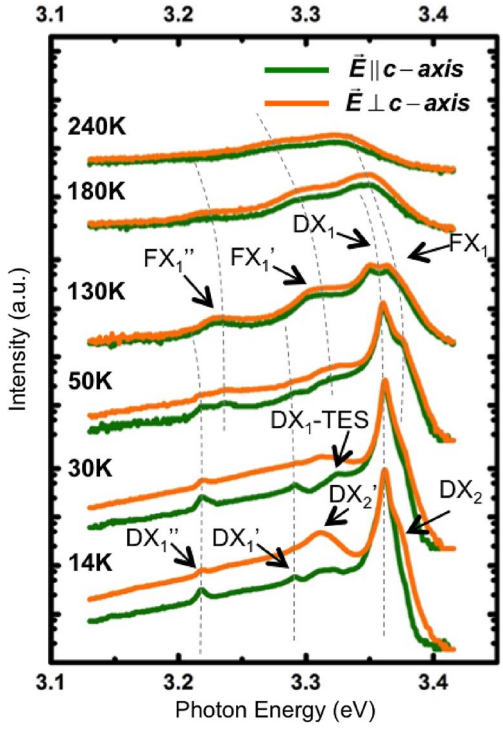


Fig. 2. Temperature dependent PL spectrum of our m-plane ZnO film for emission polarized in $\vec{E} \| c$(green) and $\vec{E} \perp c$ (orange).

XRD $\theta$–$2\theta$ scan and in-plane $\varphi$ scan. Fig. 1(a) shows the $\theta$–$2\theta$ scan of ZnO films grown on (112)LAO substrates, showing $(1\bar{1}00)$, $(2\bar{2}00)$ peaks of ZnO and (112) peak of LAO, thus confirming that the *m*-plane ZnO was successfully grown on the (112)LAO substrate [10]. Based on the $(2\bar{2}00)$ peak at 66.55°, the corresponding strain $\varepsilon_{yy}$ along out of plane direction can be evaluated as $-0.21\%$. Fig. 1(b) shows the in-plane $\varphi$ scan of the ZnO film, indicating two-fold symmetry, which suggests the epitaxial growth of *m*-plane ZnO films on (112)LAO [10]. More detailed materials characterizations for epitaxial *m*-plane ZnO film on (112)LAO can be found elsewhere [8].

To further confirm on the strain condition in the ZnO film on (112)LAO, the Raman spectrum was measured. In Fig. 1(c), the Raman shift of ZnO $E_{2-high}$ mode, the mode for accurate determination of the strain components, [11] is red-shifted for 2 $cm^{-1}$ as compared with that of the strain-free ZnO nanorods. By using the stiffness constant and phonon deformation potential of ZnO reported in previous literatures, the strain along $[11\bar{2}0]$ and [0001] is calculated [12], [13]. The strain $\varepsilon_{xx}$ $(\perp c)$ and $\varepsilon_{zz}$ $(\| c)$ are 0.12% and 0.27%, respectively. This result indicates the tensile strain along *c*-axis is larger, in accordance with the lattice match of 2.8% $(\| c)$ and 1.0% $(\perp c)$.

## 4. Temperature and Polarization Dependent Photoluminescence Spectra

To investigate the optical emission properties of the tensile-strained *m*-plane ZnO, we measured the PL spectrum of the *m*-plane ZnO film on (112)LAO, as shown in Fig. 2. We identified the origins of the emission peaks observed in PL spectra by varying the temperature and polarization. The optical anisotropy in non-polar ZnO can be attributed to the splitting of VBs. For wurtzite structure, the *p*-like VB splits into three subbands due to crystal field interaction and spin orbital interaction. These three subbands with the symmetry of $\Gamma_9$, $\Gamma_7$, and $\Gamma_7$ has their own selection rule of the emission polarization parallel to $[11\bar{2}0]$(a-axis), $[1\bar{1}00]$ (m-axis) and [0001] (c-axis), in

the order of increasing transition energy [14], [15]. The top two subband energy separation is only 5 meV, which are mainly mixed with $[1\bar{1}00]$ and $[11\bar{2}0]$ polarized subbands $(|X \pm iY\rangle)$. The energy separation between [0001] polarized subband $(|Z\rangle)$ and the first top subband $|X \pm iY\rangle$ is about 43 meV [16]. As a result, in *c*-plane ZnO, $[1\bar{1}00]$ and $[11\bar{2}0]$ polarized subbands have similar electron-hole pair recombination probabilities and thus low anisotropy in light emission, while the emission from [0001] polarized state is forbidden for surface emitting [8]. On the other hand, for non-polar *m*-plane ZnO, the $[1\bar{1}00]$ polarized state is forbidden for surface emitting and since the energy separation between [0001] and $[11\bar{2}0]$ polarized state is large, the $[11\bar{2}0]$ polarized state dominates in light emission, leading to the anisotropy in light emission for non-polar *m*-plane ZnO.

As shown in Fig. 2, the orange line presents the component of emission light polarized perpendicularly to the *c*-axis of ZnO $(\vec{E} \perp c)$ and the green line presents the component of the emission light polarized parallel to the *c*-axis of ZnO $(\vec{E} \| c)$. Before gaining an insight into optical anisotropy of *m*-plane ZnO films on (112)LAO, the origin of the emission peaks is discussed first. For the temperatures below 130 K, the near band edge emission is dominated by a peak at 3.362 eV, which is assigned to a donor bound exciton $(DX_1)$ due to thermal quenching characteristics [17]. Note that the suffix "1" in $DX_1$ indicates an emission originates from VBs with specific band structure. The first and second phonon replica ($DX_1'$ and $DX_1''$) and the two-electron satellites transition related to $DX_1$ $(DX_1 - TES)$ can be observed for $\vec{E} \| c$ at 3.291 eV, 3.218 eV, and 3.325 eV, respectively [16], [17]. These assignments are made according to both the difference in photon energy that equals to the energy of longitudinal optical phonon in ZnO and the similar temperature-dependent behavior associated with $DX_1$. The latter inference is based on the fact that as the donor bound excitons are thermally dissociated, the related emission, $DX_1$, $DX_1'$, $DX_1''$ and $DX_1 - TES$, are weakened simultaneously [16], [17]. In other words, as the temperature increases, the donor bound excitons gradually gain enough energy to overcome the binding energy of the donor defect state and thus become free excitons (FX). In our case, when the temperature becomes larger than 130 K, the peak at 3.377 eV begins to dominate; we assign this peak and another two peaks at 3.315 eV and 3.241 eV to be free exciton, $FX_1$, and its phonon replicas, $FX_1'$ and $FX_1''$ [17]. This assignment of emission peaks is based on the fact that optical anisotropy in the polarization of $FX_1$ and $DX_1$ is similar, which implies that these two transitions originate from excitons recombining at the VBs with similar band structures.

In our *m*-plane ZnO film on (112)LAO, the expected optical anisotropy is not observed for $DX_1$, $FX_1$ and their relevant emissions. In contrast to $DX_1$ and $FX_1$ emissions, the peak at 3.310 eV and the shoulder band at the high-energy side of $DX_1$ at 14 K exhibit high optical anisotropy while the origins of these two peaks remain unknown. To extract more information and the possible VBs reordering, we define the polarization degree $\rho$, which can basically be interpreted as the polarization anisotropy, by

$$\rho = \frac{I_\perp - I_\|}{I_\perp + I_\|} \tag{1}$$

where $I_\perp$ and $I_\|$ are the peak intensities of $\vec{E} \| c$ and $\vec{E} \perp c$. Difference in polarization degree can be ascribed to the different energy separation of VBs in which the excitons recombine. In previous studies, the peak at 3.31 eV has been assigned to be the free electron-acceptor (e-A) recombination originated from the stacking fault [13], [15]; however, in our work, the peak at 3.31 eV shows thermal quenching behavior so that it is almost unable to observe for temperature above 50 K, while in previous studies, the e-A transition remains observable at room temperature [18], [19]. To clarify the origins of the peak at 3.31 eV and its shoulder band at the right of $DX_1$, polarization degree is plotted as a function of temperature in Fig. 3. Two polarization degree peaks up to near 70% related to the two unknown emission peaks appear at

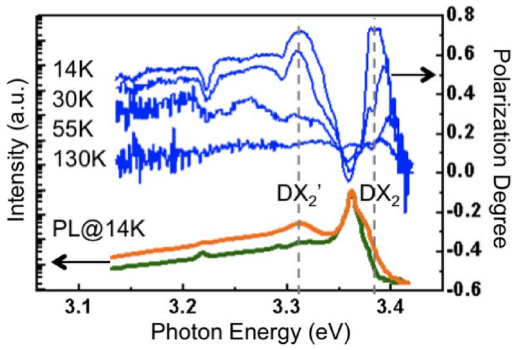


Fig. 3. Temperature dependency of polarization degree where the lower part is the PL spectrum at 14 K for comparison.

3.310 eV and 3.380 eV and decrease simultaneously as the temperature increases. Based on the similar behavior of polarization degree as a function of temperature, one can see that these two peaks originate from exciton recombination at similar VBs, which is different from $DX_1$. Since these two peaks are both thermally quenched at 50 K and the photon energy difference of these two peaks is about 72 meV, it leads us to conclude that these two peaks are donor bound excitons and that the peak at 3.31 eV is the first phonon replica of the peak at 3.38 eV, which we name as $DX_2$ and $DX_2'$.

To investigate the origins of the donors of $DX_1$ and $DX_2$, we then fit the donor binding energy of $DX_1$ and $DX_2$ using

$$I = \frac{I_0}{1 + a \bullet e^{\frac{-E_a}{kT}}} \tag{2}$$

where $I$ is the emission intensity at the temperature $T$; $I_0$ is the emission intensity at 0 K, which is approximated by the emission intensity at 14 K; $a$ is a constant; $E_a$ is the binding energy of donor; and $k$ is the Boltzmann constant [20]. The binding energy of $DX_1$ and $DX_2$ are found to be 7.0 meV and 9.0 meV, which are both close to the reported activation energy of neutral donor-bound exciton [21]–[23].

In the above study, by investigating how the polarization degree changes with the temperature, an analysis technique to study the origin of PL peaks is demonstrated. In our case, we found that $FX_1'$ and $DX_2'$ has the identical energy near 3.31 eV. Consequently, if the intensity of $DX_2'$ wasn't thermally quenched strong enough to be differentiated from $FX_1'$ under temperature variation, one may conclude these two peaks to be the same, which is wrong as one takes the difference in polarization degree of these two emission into consideration. The polarization degree reveals the information hidden in the PL spectra, as in our case, $DX_2$ in Fig. 2.

To realize the emission property with unexpected optical anisotropy in tensile-strained *m*-plane, we propose a strain-modified band structure based on the PL spectra. In the PL spectra, main emission peaks $DX_1$ and $FX_1$ have low polarization degree ($\sim$10%) at 240 K. The low polarization degree of emission is mainly due to overlapping of two VBs; therefore, we suggest that $DX_1$ originates from exciton recombination at the VBs whose two subbands polarized in [0001] and [11$\bar{2}$0] overlapped. $DX_2$ with high polarization degree up to $\sim$70%, on the other hand, originates from exciton recombination at the VBs whose two bands are separated. The two different VBs result from the thickness variation of the film. As the thickness increases, the strain is relaxed and therefore changes the band structure of VBs. $DX_1$ with stronger emission intensity originates from the surface of the film where the strain is partially relaxed, and $DX_2$ originates from the bottom part of the film near the interface between ZnO films and LAO substrates where the strain is not relaxed. The intensity of $DX_1$ is stronger than the intensity of $DX_2$ because most incident light is absorbed at the surface. Since the emission of $DX_2$ has stronger

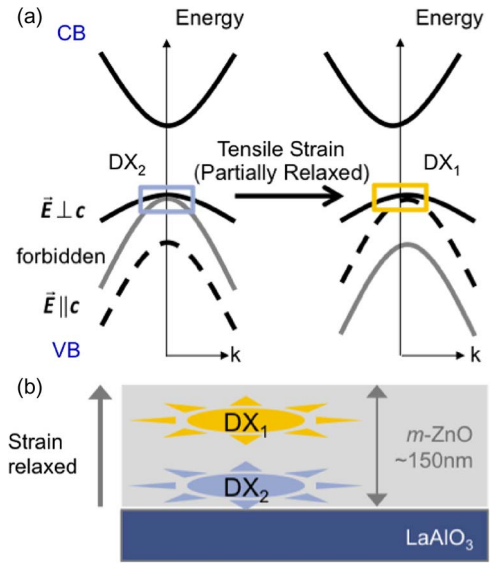


Fig. 4. Band diagram of *m*-plane ZnO with and without tensile strain.

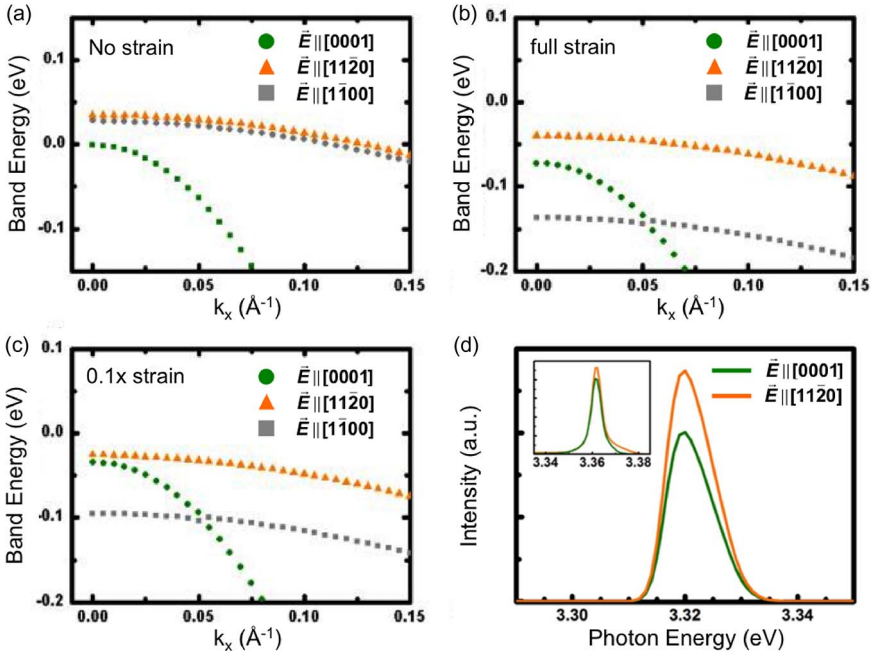


Fig. 5. Calculated valance band of (a) unstrained, (b) fully strained film, and (c) strain relaxed in $[11\bar{2}0]$ direction. (d) Simulated photoluminescence spectrum of film with strain relaxed in $[11\bar{2}0]$ direction. The inlet is the experimental PL spectrum at 14 K.

value for $\vec{E} \perp c$, we conclude that the upper subband, which has higher electron hole density, has the selection rule of $\vec{E} \perp c$. The inferred band structure reordering under tensile strain is shown in Fig. 4. The energy difference of the two subbands polarized in [0001] and $[11\bar{2}0]$ is around 40 meV under strain-free condition [16]; however, the band polarized in [0001] seems to upper shift to the position of the $[11\bar{2}0]$ polarized state in the tensile-strained ZnO film. The influence of tensile strain on the band structure of *m*-plane ZnO film is thus investigated.

## 5. Band Simulation by $k \bullet p$ Method

We further applied the $k \bullet p$ method to confirm the effect of tensile strain on *m*-plane ZnO, as shown in Fig. 5 [24], [25]. In Fig. 5(a) and (b), under the condition that the lattice mismatch are 2.8% and 1.0% along [0001] and [11$\bar{2}$0], respectively, the [0001] polarized subband has shifted closer to the [11$\bar{2}$0] polarized subband. However, as shown in Fig. 5(c), the two subbands would only be closely overlapped if the strain along [11$\bar{2}$0] is partially released, in agreement with the model we propose. Accordingly, the simulated PL spectrum in Fig. 5(d) has shown overlapped near band edge emission in the two polarization correspond to the $DX_1$ peaks in experimental spectrum. This result indicates that there are some strain relaxation mechanisms existing along the direction of [11$\bar{2}$0], which may be related to the defects [26].

## 6. Conclusion

In conclusion, through temperature- and polarization-dependent PL spectra with polarization degree analysis, we investigated the origins of each emission and related the emission properties to the VBs reordering of *m*-plane ZnO grown on (112)LAO under tensile strain. The subband polarized in [0001] in the tensile-strained ZnO *m*-plane film is found to upper shift to the position of the subband polarized in [11$\bar{2}$0], leading to the abnormal low optical anisotropy $(\rho = 10\%)$ of near band edge emission of the *m*-plane ZnO film grown on (112)LAO substrate. This study shows that to retain the desired optical anisotropy of emission, the strain in film must be taken into serious consideration.

## References


[1] A. Ohtomo, K. Tamura, and M. Kawasaki, "Room-temperature stimulated emission of excitons in ZnO/(Mg,Zn)O superlattices," *Appl. Phys. Lett.*, vol. 77, no. 14, pp. 2204–2206, 2000.

[2] D. J. Rogers *et al.*, "Electroluminescence at 375 nm from a ZnO/GaN:Mg/c-$Al_2O_3$ heterojunction light emitting diode," *Appl. Phys. Lett.*, vol. 88, no. 14, 2006, Art. ID. 141918.

[3] S. F. Chichibu *et al.*, "Effective band gap inhomogeneity and piezoelectric field in InGaN/GaN multiquantum well structures," *Appl. Phys. Lett.*, vol. 73, no. 14, pp. 2006–2008, Mar. 1998.

[4] J.-M. Chauveau *et al.*, "Growth of non-polar ZnO/(Zn,Mg)O quantum well structures on R-sapphire by plasma-assisted molecular beam epitaxy," *J. Crystal Growth*, vol. 301/302, pp. 366–369, Apr. 2007.

[5] J.-M. Chauveau *et al.*, "Non-polar a -plane ZnMgO/ZnO quantum wells grown by molecular beam epitaxy," *Semicond. Sci. Technol.*, vol. 23, no. 3, p. 35005, 2008.

[6] N. J. Diorio, M. R. Fisch, and J. L. West, "Filled liquid crystal depolarizers," *J. Appl. Phys.*, vol. 90, no. 8, pp. 3675–3678, 2001.

[7] E. C. Vail *et al.*, "Depolarized semiconductor laser sources," U.S. Patent 6760151 B1, 2004.

[8] T. Koida *et al.*, "Radiative and nonradiative excitonic transitions in nonpolar (11$\bar{2}$0) and polar (000$\bar{1}$) and (0001) ZnO epilayers," *Appl. Phys. Lett.*, vol. 84, no. 7, p. 1079, Feb. 2004.

[9] H. Matsui and H. Tabata, "In-plane anisotropy of polarized photoluminescence in M-plane (1010) ZnO and MgZnO/ZnO multiple quantum wells," *Appl. Phys. Lett.*, vol. 94, no. 16, Apr. 2009, Art. ID. 161907.

[10] Y.-T. Ho *et al.*, "Substrate engineering of LaAlO3 for non-polar ZnO growth," *Thin Solid Films*, vol. 518, no. 11, pp. 2988–2991, Mar. 2010.

[11] S. Tripathy, S. J. Chua, P. Chen, and Z. L. Miao, "Micro-Raman investigation of strain in GaN and AlxGa$_{1-x}$N/GaN heterostructures grown on Si(111)," *J. Appl. Phys.*, vol. 92, no. 7, pp. 3503–3510, Oct. 2002.

[12] I. R. Shein, V. S. Kiiko, Y. N. Makurin, M. A. Gorbunova, and A. L. Ivanovskii, "Elastic parameters of single-crystal and polycrystalline wurtzite-like oxides BeO and ZnO: Ab initio calculations," *Phys. Solid State*, vol. 49, no. 6, pp. 1067–1073, Jun. 2007.

[13] T. Gruber *et al.*, "Influences of biaxial strains on the vibrational and exciton energies in ZnO," *J. Appl. Phys.*, vol. 96, no. 1, pp. 289–293, Jun. 2004.

[14] J. Birman, "Polarization of fluorescence in CdS and ZnS single crystals," *Phys. Rev. Lett.*, vol. 2, no. 4, pp. 157–159, Feb. 1959.

[15] D. Reynolds *et al.*, "Valence-band ordering in ZnO," *Phys. Rev. B*, vol. 60, no. 4, pp. 2340–2344, Jul. 1999.

[16] B. K. Meyer *et al.*, "Bound exciton and donor-acceptor pair recombinations in ZnO," *Phys. Status Solidi*, vol. 241, no. 2, pp. 231–260, Feb. 2004.

[17] A. Teke *et al.*, "Excitonic fine structure and recombination dynamics in single-crystalline ZnO," *Phys. Rev. B*, vol. 70, no. 19, Nov. 2004, Art. ID. 195207.

[18] M. Schirra *et al.*, "Stacking fault related 3.31-eV luminescence at 130 meV acceptors in zinc oxide," *Phys. Rev. B*, vol. 77, no. 12, Mar. 2008, Art. ID. 125215.

[19] M. Schirra *et al.*, "Acceptor-related luminescence at 3.314 eV in zinc oxide confined to crystallographic line defects," *Phys. B Condens. Matter*, vol. 401/402, pp. 362–365, Dec. 2007.

[20] D. H. Chi, L. T. T. Binh, N. T. Binh, L. D. Khanh, and N. N. Long, "Band-edge photoluminescence in nanocrystalline ZnO:In films prepared by electrostatic spray deposition," *Appl. Surf. Sci.*, vol. 252, no. 8, pp. 2770–2775, Feb. 2006.
[21] M. Al-Suleiman *et al.*, "Photoluminescence properties: Catalyst-free ZnO nanorods and layers versus bulk ZnO," *Appl. Phys. Lett.*, vol. 89, no. 23, 2006, Art. ID. 231911.
[22] D. Sentosa *et al.*, "Temperature dependent photoluminescence studies of ZnO thin film grown on (111) YSZ substrate," *J. Crystal Growth*, vol. 319, no. 1, pp. 8–12, Mar. 2011.
[23] T. Sahoo *et al.*, "Photoluminescence properties of ZnO thin films grown by using the hydrothermal technique," *J. Korean Phys. Soc.*, vol. 56, pp. 809–812, 2010.
[24] S. Ghosh, P. Waltereit, O. Brandt, H. Grahn, and K. Ploog, "Electronic band structure of wurtzite GaN under biaxial strain in the M plane investigated with photoreflectance spectroscopy," *Phys. Rev. B*, vol. 65, no. 7, Jan. 2002, Art. ID. 075202.
[25] J. Wrzesinski and D. Fröhlich, "Two-photon and three-photon spectroscopy of ZnO under uniaxial stress," *Phys. Rev. B*, vol. 56, no. 20, pp. 13087–13093, Nov. 1997.
[26] W.-L. Wang, Y.-T. Ho, K.-A. Chiu, C.-Y. Peng, and L. Chang, "Structural property of m-plane ZnO epitaxial film grown on LaAlO3 (112) substrate," *J. Crystal Growth*, vol. 312, no. 8, pp. 1179–1182, Apr. 2010.